CONTINUOUS REAL-TIME SNOW PROPERTIES WITH GROUND PENETRATING RADAR

Hans-Peter Marshall[1] and Mark Robertson[1]

[1]Center for Geophysical Investigation of the Shallow Subsurface, Boise State University, Boise, ID, USA

ABSTRACT: Measurements of snow water equivalent (SWE) are important for multiple user groups, but the technology for operational continuous collection has not improved for several decades. Although recent advancements in sensor technology have been made, including radar systems, high sensor costs and other limitations have suppressed wide scale adoption. New radar hardware from Flat Earth, Inc., is relatively inexpensive and suitable for remote deployment. We combined this radar with automatic processing and deployed it at several sites for the 2016 winter. The accuracy of the radar is established with comparison profiles of manual snow pits, and tower-based continuous measurements are compared to a National Resources Conservation Service (NRCS) Snow Telemetry (SNOTEL) site, as well as to a precipitation gauge. The radar measured within $2 \pm 8\%$ SWE as compared to the manual snow pits, and was highly correlated with both the SNOTEL site and precipitation gauge.

KEYWORDS: snow water equivalent, radar, precipitation, continuous, real time

1. INTRODUCTION

Accurate measurements of SWE have implications for water resource managers, avalanche forecasters, recreationists and others. Meaningful measurements of SWE in alpine areas require sensors that are rugged, deployable in remote areas, have low power requirements and transmit in real time. Traditional technology, such as the snow pillow used by the NRCS SNOTEL sites, is relatively expensive and limited by ground improvement requirements for the pillow operation. Several new technologies for remotely measuring SWE have become available in recent years, including load cell (Johnson et al., 2015), gamma ray (Wright et al., 2011) and GPS signals (McCreight et al., 2014). However, there are limitations for each, including bridging and heat flux errors for load cells, significant calibration requirements for gamma ray and sensitivity to liquid water for GPS which have precluded widespread adoption.

Radar has been successfully applied to snow measurement applications for decades (e.g., Ellerbruch et al., 1980; Marshall and Koh, 2008), including full winter seasons (e.g., Heilig et al., 2015) but has also seen limited operational use because available radar hardware has been prohibitively expensive, is not suited for remote deployment and real time processing is difficult.

Recently available radar hardware from Flat Earth, Inc., which was designed to measure snow depth underneath snow grooming equipment, has been combined with an automatic processing algorithm, which clears the previous hurdles and has been successfully deployed during the winter season. Tower-mounted, downward-looking Flat Earth radar has been deployed at several sites. These include the NRCS Banner Summit SNOTEL site near Stanley, Idaho, USA, where it is co-located over the SNOTEL pillow, and the Garden Mountain weather station, approximately 10 km northeast of Banks, Idaho, USA, where it is within several meters of a precipitation gauge.

The accuracy of the radar is described by a series of 15 focused profiles over snow pits, and comparison with the Banner Summit SNOTEL and Garden Mountain weather station.

2. THEORY

Since the radar is mounted at a known height, once the snow and ground surface reflections are identified the snow depth, radar velocity and real permittivity are known by

$$v = \frac{2z}{twt} = \frac{C}{\sqrt{\varepsilon_s'}} \quad (1)$$

where v is the radar velocity, z is the snow depth, twt is the two way travel time between reflections, ε_s' is the real permittivity of the snow and C is the speed of light.

Liquid water causes frequency-dependent attenuation of radar, and the spectral shift method (Bradford, 2009) uses the difference in instantaneous frequency between the snow surface and ground surface reflections to calculate the imaginary component of the permittivity of the snow, ε_s''. Once ε_s'' is known the percent by volume liquid water content, W, and snow density, ρ_d, can be

calculated from well-established empirical relationships (Tiuri et al., 1984)

$$\varepsilon'_d = (1 + 1.7\rho_d + 0.7\rho_d^2) \quad (2)$$

$$\varepsilon'_s = (0.1W + 0.8W^2)\varepsilon'_w + \varepsilon'_d \quad (3)$$

$$\varepsilon''_s = (0.1W + 0.8W^2)\varepsilon''_w \quad (4)$$

where $\varepsilon'_w + i\varepsilon''_w$ is the complex permittivity of water.

The radar has an on-board microprocessor which performs radar trace processing and an algorithm that identifies the snow and ground surfaces in the radar trace and makes calculations of SWE,

$$SWE = z(\rho_d + W). \quad (5)$$

3. RESULTS

The performance of the radar was evaluated directly over a series of 15 snow pits. For these measurements a brief radar profile was taken over an ~1 m^2 snow surface. A snow pit was subsequently excavated and manual measurements of snow depth, density, SWE and, when appropriate, liquid water content with a Snow Fork (Sihvola et al., 1986) were collected.

Using independent measurements of snow depth from the snow pit, the radar measured density was within the range of uncertainty in manual density estimates (Proksch, 2016) for 12 of the 15 pits (Fig. 1).

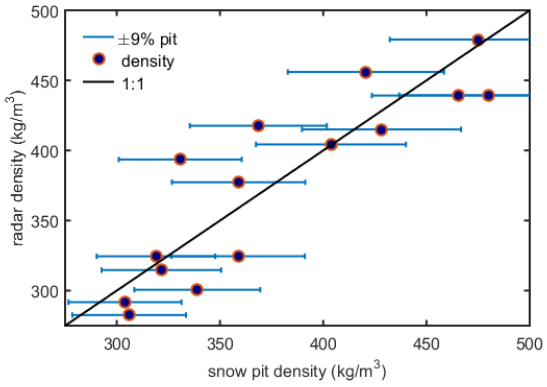

Fig. 1: Using snow pit measurements of depth, radar calculations of density are compared with pit density over a series of 15 pits. Error bars on the manual snow pit density are $\pm 9\%$. For 12 of the 15 pits the radar density was within $\pm 9\%$ of the manual density.

Since SWE is a function of snow density, errors in the radar measurements of SWE followed those of density (Fig. 2). Radar-derived SWE was within the uncertainty of the manual measurements, $\pm 9\%$ density multiplied by depth, for 12 of the 15 pits. There was a slight positive bias in radar-derived SWE, as across all 15 snow pits the percent error in SWE was $2 \pm 8\%$, and the absolute percent error was $6 \pm 5\%$. It is instructive to consider the consequences of choosing an arbitrary density measurement to the range of observed depths. In this case, if a single arbitrary density of 320 $\mathrm{kg\ m^{-3}}$ is applied, the number of radar measurements that fall within the uncertainty of the manually derived SWE drop from 12 to 5.

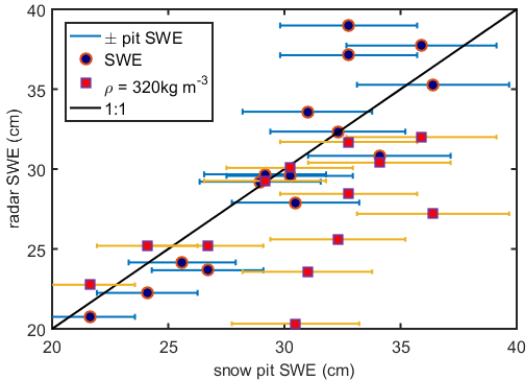

Fig. 2: Using snow pit measurements of depth and radar measurements of density, radar calculations of SWE are compared with pit SWE for the same series of 15 pits as in Fig. 1. Error bars for the manual SWE are $\pm 9\%$ multiplied by the pit depth. For 12 of the 15 pits the radar SWE was within the uncertainty of the manual measurements. Red squares shown the consequences of an arbitrarily chosen density, in this case 320 $\mathrm{kg\ m^{-3}}$, applied to the independent depth measurements.

Tower-mounted, downward looking radar measurements were collected at the Banner Summit SNOTEL and Garden Mountain weather station for significant portions of the 2016 winter season. Radar measurements were made at 15 minutes intervals. Although real-time data transmission did not occur at either site, the results were processed using an algorithm that functions in real-time, outputs SWE values, and could be expected to perform similarly when transmitting data in real time.

The Banner Summit SNOTEL is at an elevation of 2145 m. Radar measurements began on January 14th, 2016, and data through April 12th is presented. Observed SWE values ranged from 36 - 75 cm as measured by the SNOTEL and from 36 – 84 cm as measured by the radar (Fig. 3).

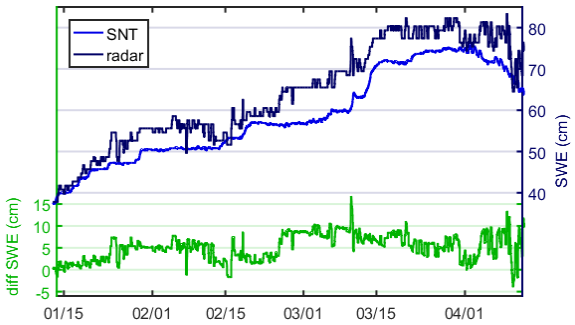

Fig. 3: Results from the radar (black) and Banner Summit SNOTEL (blue) from January 14th-April 12th, 2016, and well as the difference in SWE between the two measurements (green) are shown.

For the period from February 12th – 16th, radar-derived SWE estimates drop approximately 5 cm. This drop was not seen in the SNOTEL SWE value and occurred during a period that was cold enough that significant melt was not a factor. The drop in radar-derived SWE was caused by the automatic algorithm misidentifying the ground surface reflection. After several days of erroneous calculations, the algorithm corrected itself to reasonable values.

After the initial accumulation period in late January the radar generally overestimates SWE compared to the pillow. Since snow bridging and underestimates of SWE are known to occur, it is possible that the positive bias in radar SWE estimates are actually the more accurate measurement of snow on the ground.

Despite the approximately four day period of error in mid-February, radar and SNOTEL SWE values were highly correlated, with a R^2 of 0.97 (Fig. 4).

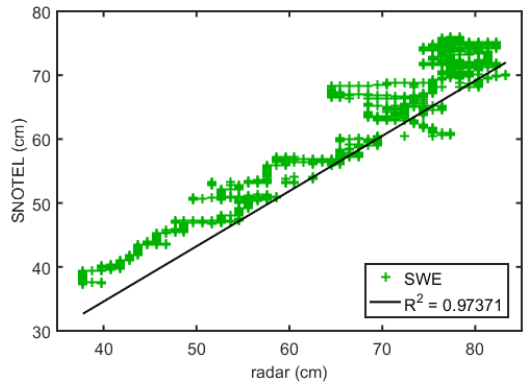

Fig. 4: Radar-derived SWE values were highly correlated with SNOTEL values, with R^2 of 0.97.

The Garden Mountain weather station is located at an elevation 2040m elevation in the west central Idaho Mountains, approximately 10 km northeast of Banks, Idaho. There is not a direct measurement of SWE at the site, but radar values are compared to a high resolution precipitation gauge.

Radar measurements at the Garden Mountain weather station were collected from December 16th, 2015 through March 5th, 2016, over a range of 30 – 45 cm SWE as measured by the radar (Fig. 5). The prominent spike in SWE in mid-February, and subsequent drop, occurred during a period of densification immediately following an accumulation event and warm period. The cause of the spike is not completely known, but may be related to rime or snow on the radar antenna.

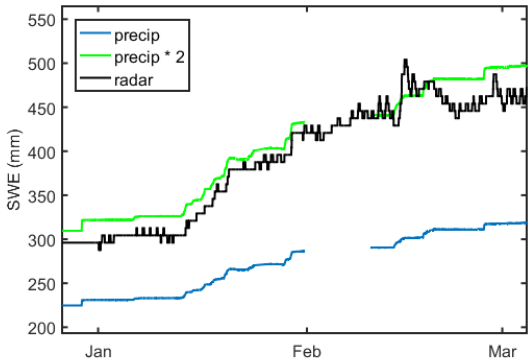

Fig. 5: Radar-derived water equivalent (black), precipitation gauge water equivalent (blue), and a factor of two applied to the precipitation gauge (green) at the Garden Mountain weather station.

Radar and precipitation gauge water equivalent values were also highly correlated, with a R^2 of 0.94 (Fig. 6).

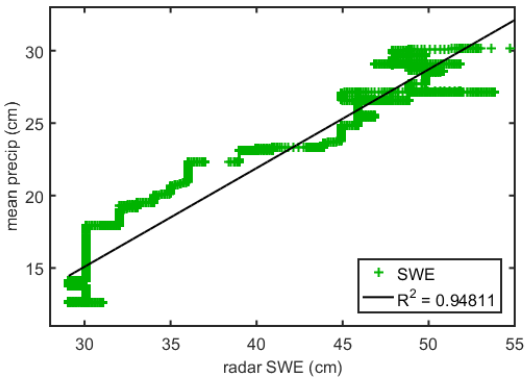

Fig. 6: Radar-derived water equivalent values were highly correlated with precipitation gauge values, with a R^2 of 0.94.

4. CONCLUSION

The Flat Earth radar system successfully measured SWE in remote locations and, although it was not completed in time for application during the 2016 winter season, the data was processed with an automatic algorithm that is appropriate for real-time application.

The radar system was proven to be accurate to within $2 \pm 8\%$ of manual snow pits in a series of 15 snow pits. Subsequent winter season deployments were also successful. The radar followed bulk SWE trends as measured by a snow pillow at the Banner Summit SNOTEL site, where SWE values were highly correlated with a R^2 of 0.97 and nearly all radar-derived SWE measurements were within +10 cm as measured by the pillow. The radar was also highly correlated with precipitation gauge measurements of water equivalent at the Garden Mountain weather station, with a R^2 of 0.94. As further improvements are made with the real time processing, which will eliminate the short periods of erroneous SWE estimates at both the Banner Summit SNOTEL and Garden Mountain weather station sites, the Flat Earth radar system could prove to be an extremely useful tool for remotely measuring SWE.

REFERENCES

Bradford, J., J. Harper, J. Brown, 2009: Complex dielectric permittivity measurements from ground-penetrating radar to estimate snow liquid water content in the pendular regime. *Water Resources Research,* 45, W08403.

Johnson, J., A. Gelvin, P. Duvoy, G. Schaefer, G. Poole, G. Horton, 2015: Performance characteristics of a new electronic snow water equivalent sensor in different climates. *Hydrological Processes*, 29, 1418-1433.

Ellerbruch, D., H. Boyne, 1980: Snow stratigraphy and water equivalence measured with an active microwave system. *Journal of Glaciology*, 26, 225-233.

Heilig, A., C. Mitterer, C. Schmid, N. Wever, J. Schweizer, HP Marshall, O. Eisen, 2015: Seasonal and diurnal cycles of liquid water in snow – measurements and modeling. *Geophysical Research Letters: Earth Surface*, 120(10), 2139-2154.

Marshall, H.P., G. Koh, 2008: FMCW radars for snow research. *Cold Regions Science and Technology*, 52(2), 118-131.

McCreight, J.L., E. Small, K. Larson, 2014: Snow depth, density, and SWE estimates derived from GPS reflection data: Validation in the western U.S. *Water Resources Research*, 50(8), 6892-6909.

Proksch, M., N. Rutter, C. Fierz, M. Schneebeli, 2016: Intercomparison of snow density measurements: bias, precision and vertical resolution. *The Cyrosphere*, 10, 371-384.

Sihvola, A., M. Tiuri, 1986: Snow fork for field determination of the density and wetness profiles of a snow pack. *IEEE Transactions on Geoscience and Remote Sensing*, GE-24 (5), 717-721.

Tiuri, M., A. Sihvola, E. Nyfors, M. Hallikaiken, 1984: The complex dielectric constant of snow at microwave frequencies. *IEEE Journal of Oceanic Engineering*, 5, 377-382.

Wright, M., J. Kavanaugh, C. Labine, 2011: Performance Analysis of GMON3 Snow Water Equivalency Sensor. Proceedings of the *Western Snow Conference*, Stateline, NV.